Ramjets: Airframe Integration

Jean-Luc Moerel, Wouter Halswijk
TNO Defence, Security and Safety
Lange Kleiweg 137
2280 AA Rijswijk
The Netherlands

jean-luc.moerel@tno.nl

wouter.halswijk@tno.nl

ABSTRACT

These notes deal with the integration of a (sc)ramjet engine in either an axisymmetric or a waverider type of cruise missile configuration. The integration aspects relate to the integration of the external and internal flow paths in geometrical configurations that are being considered worldwide. Integration of these two flow paths combined with the vehicle concept that flies an equilibrium cruise flight (lift = weight and thrust = drag) has led to an evaluation tool, HyTEC (Hypersonic Technology Evaluation Code) that estimates the system performance parameter cruise flight range as function of design options: vehicle concept (axisymmetric or waverider) and scale, ramjet or scramjet propulsion and mission options (e.g. flight speed, flight altitude). First-order engineering relations for the aerodynamic and propulsive forces in the supersonic and hypersonic flight regime constitute the basis of this tool. The notes are structured as follows: after the introduction the evaluation tool HyTEC and typical analysis results are discussed. Next the results of a case study are given and finally the notes deal with some first steps to improve HyTEC. Most of the contents of these notes are more extensively described in references 1, 2 and 3.

1.0 INTRODUCTION

Defence, Security and Safety is one of the five core areas of TNO (abbreviation for 'Netherlands Organisation for Applied Scientific Research'). Under this header TNO supports the Ministry of Defence in all its activities. The work presented in these notes is aimed at gaining insight in world-wide technology developments for future high speed long range weapon systems. It serves as a starting point for the development of Modelling & Simulation tools which are required to accurately predict high speed long range weapon system performance in the future. This prediction capability will be used to support the Armed Forces during weapon acquisition programs and assessments of their defence capability against threats.

Many countries are working on the development of hypersonic air breathing cruise missiles (with cruising speeds of Mach 4 and higher). They are foreseen to be employed against, amongst others, deeply buried targets. The main technological challenges are related to severe aerodynamic heating and complex physical processes of aerodynamics and combustion at hypersonic flight speeds.

These notes report on a study of the cruise flight dynamics of high speed long range weapon systems. The focus of the study lies on understanding the gas dynamics of both the external flow (inducing aerodynamic lift and drag) and internal flow (for generation of thrust).

A system engineering tool called HyTEC (Hypersonic Technology Evaluation Code) was developed for conducting cruise flight performance analyses of hypersonic air breathing cruise missiles. Two baseline cruise weapon configurations (an axi-symmetric and a waverider configuration) were defined for these system performance analyses. The system engineering tool calculates the cruise flight range of these systems. It can be shown that the cruise flight range is proportional to the product of flight speed, specific

impulse of the motor, the aerodynamic lift over drag ratio and fuel to overall system mass ratio. Engineering methods for the prediction of aerodynamic lift and drag, and ramjet and scramjet propulsion characteristics are described and vehicle integration aspects of aerodynamics and propulsion are included in HyTEC.

Two kinds of evaluations can be performed using the system engineering tool HyTEC: the evaluation of the influence of design choices on system performance and the evaluation of the effect of model uncertainties on system performance. These evaluations help to understand design choices that are being considered for hypersonic cruise missiles. By revealing the model parameters that influence system performance most, critical technologies can be identified.

2.0 DESCRIPTION OF HYTEC AND TYPICAL ANALYSIS RESULTS

2.1 Hypersonic Air Breathing Cruise Missile Configurations

The definition of baseline weapon configurations has been based on, amongst others, information on world-wide development programs of hypersonic air breathing cruise missiles [1, 2]. This description of the baseline cruise weapon configurations concerns mission characteristics (including cruise flight speed, flight profile and range), propulsion characteristics and vehicle integration characteristics (vehicle shape, dimensions and mass).

2.1.1 Mission characteristics

The first missions of hypersonic cruise weapon systems will probably focus on destroying fixed targets like airports and bunkers from a stand-off distance of 1000 km and higher. The cruise weapon system will be launched from the ground or an airplane and subsequently accelerate and climb by means of rocket propulsion. A (sc)ramjet motor takes over the propulsion at a certain appropriate flight speed. At 30km altitude, the missile will cruise over a large distance (1000 km typically) with cruise flight speeds between Mach 4 and 8. Finally, the missile will descend towards its target.

2.1.2 Propulsion characteristics

The cruise flight has been analyzed by assuming operation of either a ramjet or a scramjet motor. A hydrocarbon type of fuel is assumed because of the focus on military applications and the presumed benefit of ‘one fuel on the battlefield’.

2.1.3 Vehicle integration characteristics

Two external shapes of cruise weapon configurations are considered: an axi-symmetric weapon body with a nose air intake and wings and fins for aerodynamic lift and control (e.g. HyFly, Figure) and a waverider type of weapon body (rectangular or elliptical-like cross-sections) with the air intake at the lower side of the weapon body and wings and fins for aerodynamic lift and control (e.g. X-51, Figure 2). Figure 3 gives the generalized representations of both the waverider and axisymmetric type missile configurations.

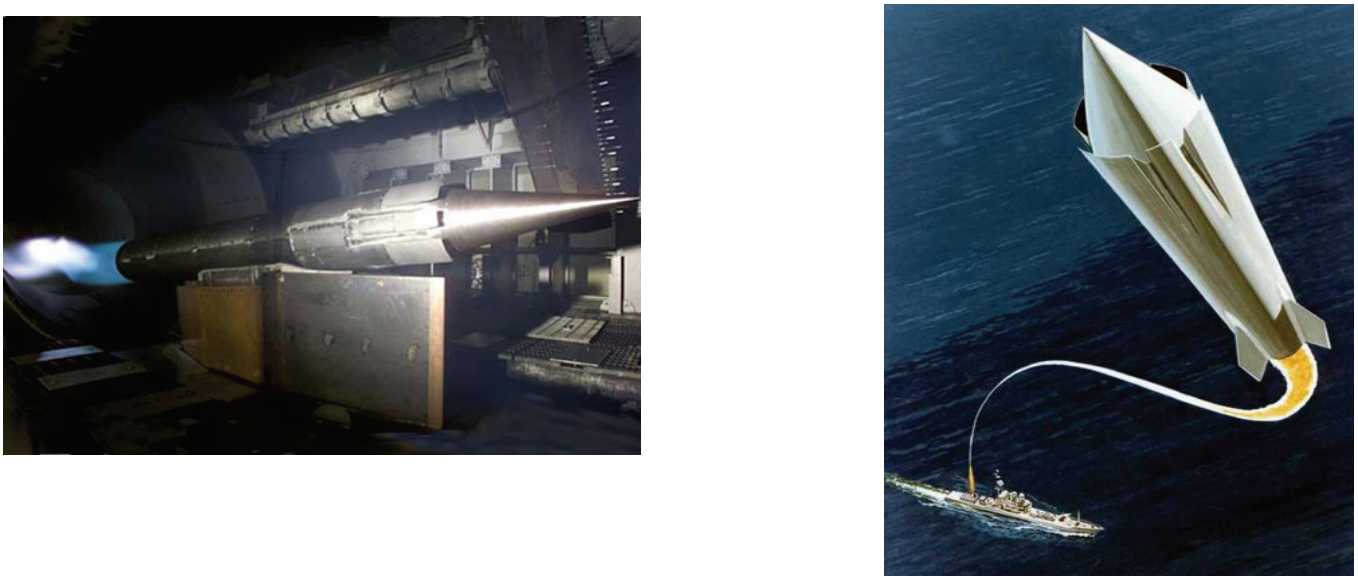

Figure 1 Axisymmetric type missile configuration: Hypersonics Flight Demonstration program (HyFly)

Figure 2 Wave rider type missile configuration: The X-51 Waverider, attached to the underbelly of a B-52 long-range bomber *(Wright-Patterson AFB photo gallery / Chad Bellay / United States Air Force)*

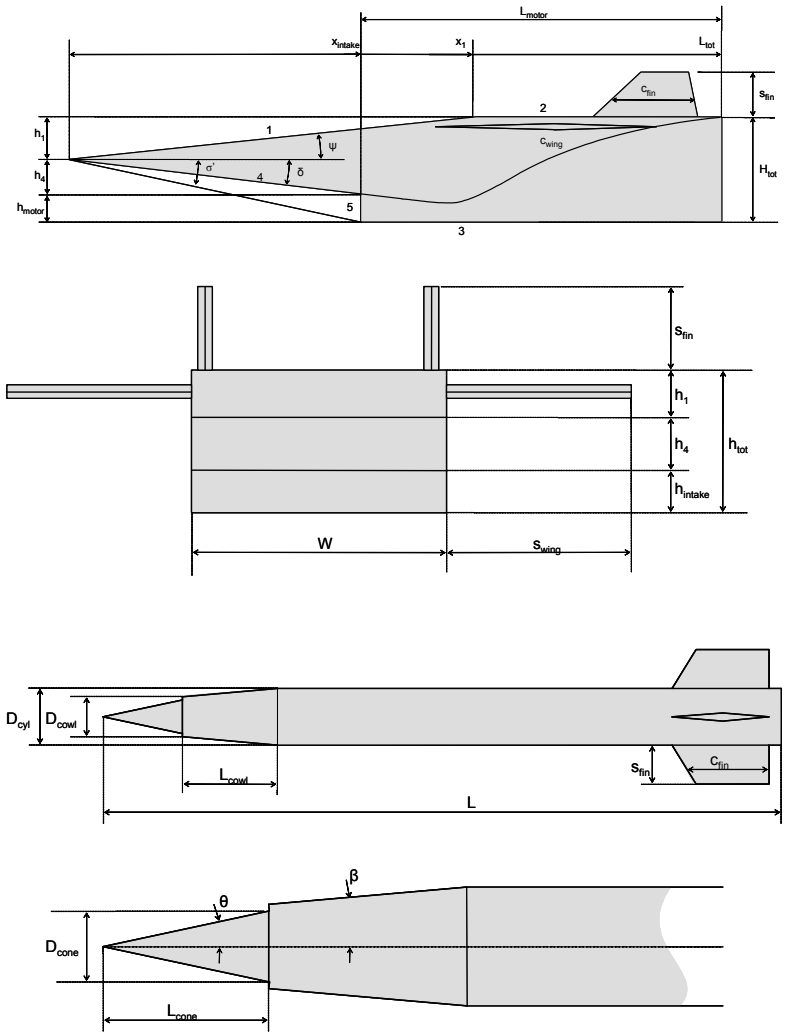

Figure 3 Generalized representations of the waverider and axisymmetric type missile configurations as used by HyTEC

The overall dimensions of the baseline cruise weapon configurations have been estimated based on the assumption of carriage by air based launch platforms (e.g. fighter planes). This implies that they can neither be extremely large, nor extremely heavy:

- Length of 4m (without booster)
- Diameter of 0.4m (axi-symmetric configuration)
- Cross-sectional height and width of 0.314m and 0.4m respectively (waverider configuration)

The mass of the cruise weapon configurations is estimated in a rudimentary way by assuming a mean missile mass density of 1000 kg/m^3 [1, 2]. With the assumed geometrical dimensions of the cruise weapon configurations , both configurations have a mass of around 430kg. This estimated mass excludes the mass required for the boost phase. In order to judge upon the capability of military airplanes to carry hypersonic cruise weapon systems, this additional mass needs to be taken into account. The worst case (i.e. maximum amount of additional mass) would be the case for which a solid propellant rocket motor alone is assumed

to provide the acceleration of the weapon system from launch until the maximum envisaged cruise flight speed of Mach 8 for hypersonic cruise weapon systems. With Tsiolkovsky's rocket equation,

$$M_L = M_C * e^{\Delta V / I_{sp}}$$

the required boost propellant mass was calculated (573kg!) which results in a weapon system launch mass of 1003 kg (neglecting extra structural mass required to integrate the boost propellant with the vehicle). This launch mass is considered to be manageable by military airplanes. For example, the JASSM (Joint Air-to-Surface Standoff Missile) has a launch mass of 1020 kg and can be integrated with many U.S. strike aircraft [1, 2].

In the equation above M_L is the total vehicle mass at launch (including the booster propellant), M_C is the cruise flight vehicle mass (at start of the cruise flight: 430 kg), ΔV is the total vehicle velocity increase during the boost phase (from Mach 1 to the cruise flight Mach number) and I_{sp} is the specific impulse of the booster engine (assuming a solid propellant rocket engine with a state-of-the-art specific impulse of 250s.)

2.2 Modeling of External Aerodynamics

Aerodynamic lift and drag are important factors that influence the maximum range of the cruise weapon systems. With engineering models, these forces are predicted as function of different shapes and dimensions, Mach number, angle-of-attack and flight altitude. Figure 4 shows the aerodynamic forces acting on the cruise flight vehicle.

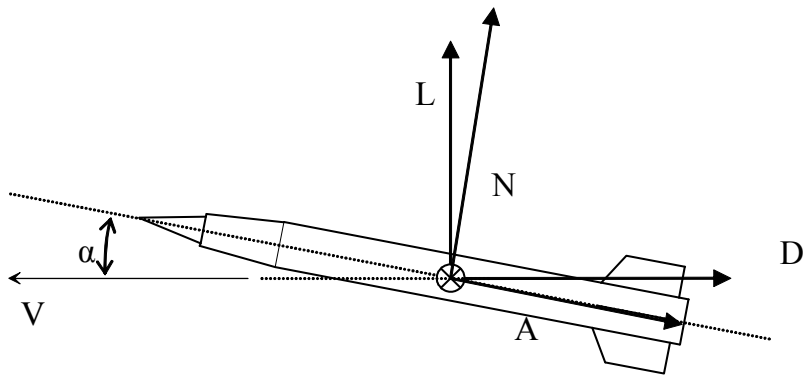

Figure 4 Lift (L) and Drag (D) or Normal force (N) and Axial force (A). Both sets are related via common basic goniometric relations

For the purpose of computing the aerodynamic forces of the axi-symmetric weapon system, the weapon configuration is broken down into the elementary geometries of a cone (inlet external compression surface and cowl), cylinder (main weapon body) and flat plates (wings and fins). Analytical engineering models for the aerodynamic lift and drag have been obtained for these elementary geometries. All elementary geometries of the axi-symmetric weapon configuration are assumed to be subjected to free stream flow conditions (i.e. no flow interference effects between the elementary geometries are taken into account) and the total lift and drag force of the entire weapon system are estimated by adding up the forces of the individual elementary geometries.

For the cylinder, the body alone normal force coefficient based on slender body theory and cross flow

theory is estimated by:

$$C_N = \sin(2\alpha)\cos(\alpha/2) + 2(l/d)\sin^2(\alpha)$$

With C_N the normal force coefficient, α, the angle-of-attack of the missile with respect to the free stream flow and l/d the length over diameter ratio of the cylinder.

The normal force coefficient for wings and fins is based on linear wing theory and Newtonian impact theory:

$$C_N = \frac{4\sin(\alpha)\cos(\alpha)}{\sqrt{M^2 - 1}} + 2\sin^2(\alpha)$$

With M, the flight Mach number.

The inviscid zero lift drag coefficient for wings and fins of both configurations based on linear wing theory is calculated as follows:

$$C_{D_0} = 5.3\frac{\left(t/c\right)^2_{\max}}{\sqrt{M^2 - 1}}$$

With C_{D0}, the zero lift drag coefficient and $(t/c)_{max}$ the maximal thickness of the wing or fin over the wing or fin chord.

The inviscid cowl drag of axi-symmetric configuration is roughly estimated based on Newtonian impact theory. Furthermore the Lift and drag of the external intake surfaces are implicitly accounted for within the control volume for the assessment of the propulsion induced forces on the vehicles (for both configurations).

Skin friction coefficients for both laminar and turbulent flow are used to account for the viscous friction force along the wetted outer surfaces of both vehicles:

$$c_f = \frac{0.664}{\sqrt{\mathrm{Re}_x}\left(\frac{T'}{T_e}\right)^{0.12}}$$

$$c_f = \frac{0.0592}{\sqrt[5]{\mathrm{Re}_x}\left(\frac{T_T'}{T_\infty}\right)^{0.648}}$$

In order to estimate the aerodynamic forces acting on the waverider weapon configuration, the system is considered to be a collection of flat surfaces. The analytical expressions for the pressure forces acting on these flat surfaces are based on the standard 2D oblique shock and Prandtl-Meyer expansion waves for supersonic flow. Flow interference between the different flat surfaces is taken into account by taking the calculated properties of the flow along a flat plate as free stream conditions for the flat surface following downstream. The contribution to the drag force by skin friction is calculated in the same way as for the axi-symmetric configuration.

2.3 Ramjet and Scramjet Propulsion Modelling

The main assumptions of the basic engineering models for propulsion performance are [1,2]:

- One-dimensional, steady flow
- No effect of angle-of-attack (the engine is assumed to be aligned with the flight velocity)
- Air flow is a perfect gas with constant caloric properties equal to those of the ambient air (γ=1.4)
- No effects of fuel mass addition ($m_f << m_a$)
- Complete combustion of the fuel yielding CO_2 and H_2O as reaction products in case of hydrocarbons as fuel (i.e. below stochiometric mixture ratios of air and fuel)
- Models are valid for design point conditions (i.e. geometry of the engine is assumed to be variable and is adapted to the design conditions such as flight Mach number, flight altitude, fuel-air ratio, intake flow etc.)
- On-design intake operation (no spillage)
- Ideal expansion ($p_e = p_0$)
- Adiabatic, non-isentropic flow in intake and nozzle
- Brayton (or Joule) cycle: combustion at constant pressure at non-zero velocity

The combustion process is modelled by means of adding heat to the internal air mass flow. With the heating value H_f per unit of fuel mass, the combustion efficiency η_B and the fuel mass flow rate m_f, this heat can be calculated as follows:

$$m_a q = \eta_B m_f H_f$$

To arrive at predictions of the performance of a ramjet or scramjet motor, the physics of the internal flow path from free stream conditions until nozzle exit conditions is modelled (see Figure 5).

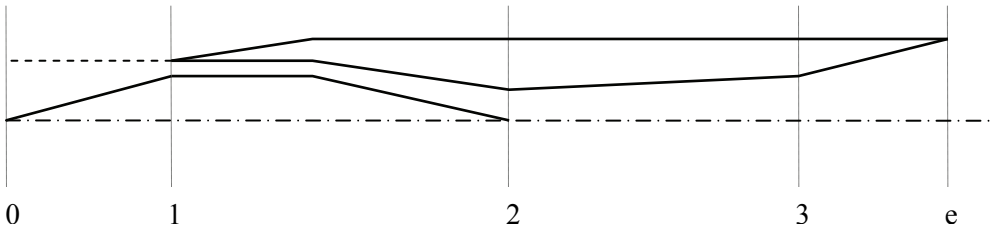

Figure 5 Internal flow path physics consisting of compression of the air (by the external compression surface, from station 0 to 1, and within the air intake, from station 1 to 2) followed by constant pressure combustion from station 2 to 3 and finally expansion within the nozzle from station 3 to e

As a consequence of the assumptions of no flow spillage by the air intake, and ideally expanded flow at the nozzle exit, the net thrust of the motor can simply be calculated as follows:

$$F_l = m_a(V_e - V_0)$$

The nozzle exit velocity of the air flow can be solved from the energy equation using the adiabatic nozzle flow assumption and can be written as follows:

$$\frac{V_e}{V_0} = \sqrt{\frac{T_{t_3}/T_0}{\frac{\gamma-1}{2}M_0^2}\left\{1-\left(\frac{p_0}{p_{t_e}}\right)^{\frac{\gamma-1}{\gamma}}\right\}}$$

with T_{t3} the total temperature at station 3 and p_{te} the total pressure at the nozzle exit. Knowing the exit velocity V_e, the specific impulse of the motor can be calculated:

$$I_{sp} = \frac{F_l}{m_f g}$$

The total temperature T_{t3}, follows from the energy equation using the heat q added to the internal air flow:

$$q = c_p(T_{t_3} - T_{t_2})$$

with T_{t2} the total temperature at station 2 which equals the total temperature of the free stream flow.

From the equation for V_e/V_0 it can be seen that the total pressure at the nozzle exit influences the exit flow velocity and consequently the overall performance of the propulsion system. The higher the total pressure (i.e. the lower the pressure losses of the internal flow physics), the better will be the performance of the propulsion system. The total pressure loss is composed of the contributions of the intake, combustion chamber and exhaust nozzle. For the intake and exhaust nozzle the total pressure losses are often expressed through kinetic efficiency factors:

$$\eta_k = \frac{(V_0)_{is}^2}{V_0^2}; \qquad \eta_n = \frac{V_e^2}{(V_e)_{is}^2}$$

In these expressions $(V_0)_{is}$ is the velocity of the air when expanded isentropically from the conditions at station 2 to the atmospheric pressure and $(V_e)_{is}$ is the velocity of the air when expanded isentropically from the conditions at station 3 to the atmospheric pressure (see 5). It can be shown that the intake kinetic efficiency factor, which is a function of the total pressure ratio p_{t2}/p_{t0}, remains approximately constant with

varying design flight Mach number for flight Mach numbers higher than Mach 4. Proper baseline values for the intake efficiency that are are η_K=0.90 and η_K=0.98 for a ramjet and scramjet motor respectively [1,2]. The intake of a scramjet causes less total pressure loss in the flow, compared with a ramjet intake. The reason for this is the fact that the flow at the end of a scramjet intake is still supersonic, contrary to a ramjet intake where the flow is decelerated to subsonic speed through a normal shock. For the nozzle, total pressure losses have not been taken into account (i.e. a kinetic efficiency factor of 1 has been assumed).

From the assumption of combustion at constant pressure, an expression for the total pressure loss inside the combustion chamber can be derived, based on the conservation laws for mass, momentum and energy [1, 2]. From this expression it follows that combustion is always accompanied by a loss in total pressure ($p_{t3} < p_{t2}$). Furthermore, it can be shown that the larger the Mach number at the end of the intake, M_2, the larger the total pressure loss inside the combustion chamber. For a ramjet motor M_2<1 and the total pressure loss is much smaller than the total pressure loss occurring within the intake. For the system analyses M_2 = 0.4 has been used. For the scramjet motor for which M_2>1, the total pressure loss occurring within the combustion chamber is significant. Low values of M_2 are beneficial for keeping the total pressure loss due to combustion low, but a lower limit must be respected due to various aerodynamic considerations (amongst others the starting behaviour of inlets). For the system analyses a minimum value of $M_2 = 0.4M_0$ has been used as baseline. This value for M_2 constitutes a minimum value that can be accomplished with an external compression intake with internal contraction [1, 2].

The fundamental models for ramjet and scramjet propulsion do not incorporate the effects of dissociation of the combustion products CO_2, H_2O and the remaining O_2 in the internal gas flow. This cannot be neglected for the higher end of the flight Mach number range, due to the very high total temperatures of the freestream flow. Dissociation is an endothermic reaction, causing a reduction of the temperature of the flow, which leads to a lower thrust.

Dissociation affects ramjets and scramjets to a different extent and therefore an engineering model for the influence of dissociation on the motor performance was conceived, in order to capture the differences between ramjet and scramjet propulsion more realistically. Figure 6 shows results of calculations of the effects of dissociation for a representative mixture ratio (one quarter of the stochiometric mixture ratio). The estimated losses of thermal energy are incorporated in the motor performance predictions as function of the ideal combustion temperature. A ramjet engine, where the air is decelerated to subsonic velocities, reaches higher static combustion chamber temperatures than a scramjet engine, where the air flow within the combustion chamber is supersonic. At a given flight speed, a ramjet engine will therefore suffer a larger performance reduction because of dissociation. This will become more pronounced at higher Mach numbers.

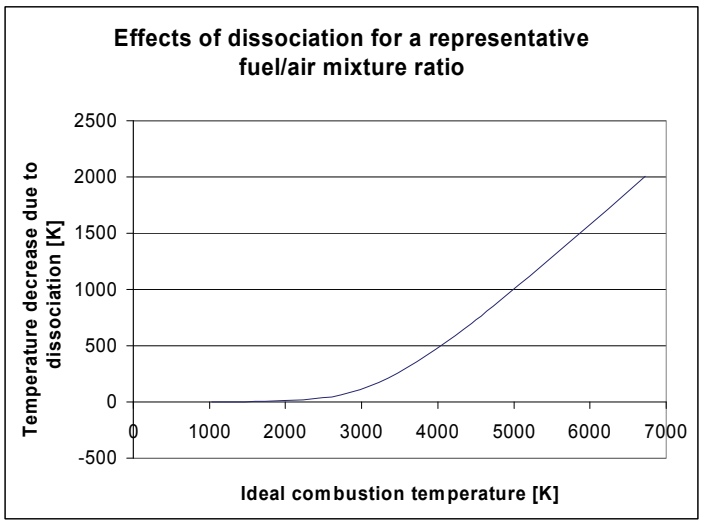

Figure 6 **Result of computations with the NASA CEA2000 chemical equilibrium code: The loss of temperature due to dissociation is plotted versus the ideal temperature due to the combustion of the compressed air flow. For ideal temperatures of 2500K and higher the effect of dissociation is significant.**

Some of the chemical energy stored in dissociated molecules may be converted back into thermal energy

in the nozzle, as the temperature drops during the expansion of the gasses. This will lead to recombination of dissociated molecules. To be able to account for the effect of recombination of the dissociated gasses in the nozzle, a parameter β is used as follows: the parameter may vary between 0 and 1 where the choice of β=0 corresponds with no recombination and β=1 with full recombination, for which it has been assumed that motor performance equals the ideal motor performance (i.e. the effects of dissociation are not taken into account). The baseline value for the parameter β has been set to 0.5.

2.4 System Integration Modelling

Vehicle system performance is evaluated using the conditions at the start of the cruise flight, at equilibrium of forces. This means that the sum of all the forces acting on the vehicle is zero. In the system engineering tool, which is programmed in MATLAB, these forces are calculated in two separate modules; the propulsion module and the aerodynamic module. In Figure 7, F_l (net thrust which is in-line with the weapon body longitudinal direction) and F_n (normal thrust force due to deflection of the internal flow) are predicted by the propulsion module. D (drag) and L (lift) are predicted by the aerodynamic module. The input for these modules consists of altitude (defining the atmospheric conditions), Mach number, geometric configuration and angle of attack. For the propulsion module, the heat parameter q/c_pT_0 is also required (which defines the fuel mass flow). To find equilibrium of forces, only the angle of attack and the heat parameter are varied.

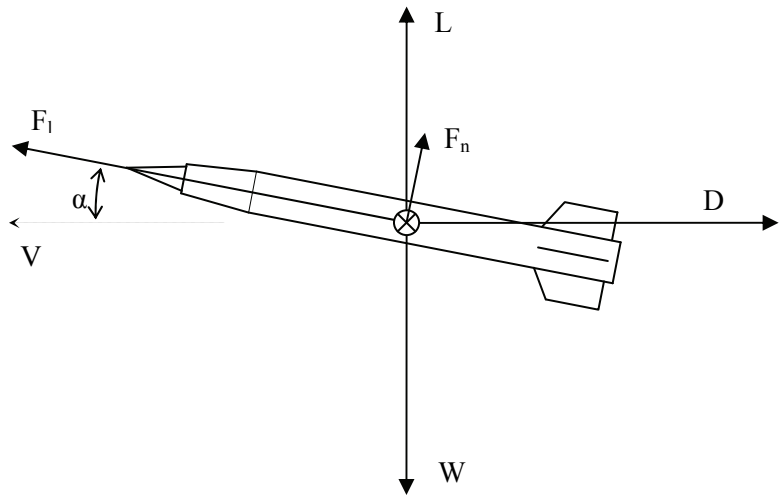

Figure 7 The forces on a vehicle in equilibrium flight

Important vehicle integration aspects that play a role within the calculations of the equilibrium of forces and the range are related to:

- The boundary between internal and external aerodynamics
- The geometrical dimensions that define the amount of air that is captured and the extent of expansion within the nozzle
- The effects of the angle-of-attack on the air capture by the inlet and on the normal force F_n due to the deflection of the internal flow (see Figure 7).

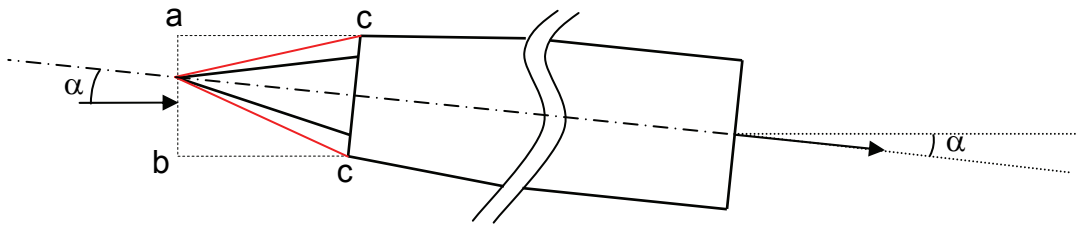

Figure 8 Internal flow path sketch for the axi-symmetric weapon configuration

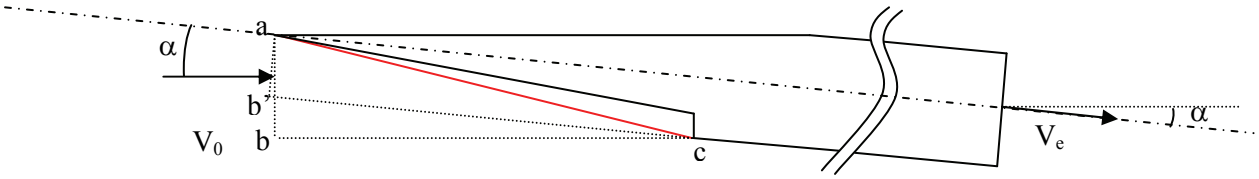

Figure 9 Internal flow path sketch for the waverider weapon configuration

The forces acting on the vehicles, caused by the internal flow and combustion processes, are evaluated using a control volume that contains the internal flow. The upstream boundary consists of a plane within the freestream and perpendicular to the freestream velocity vector. Its surface area corresponds to the inlet air capture for on-design inlet operation, for which the oblique shocks (in red) coincide with the cowl lip (designated with c in Figure 8 and Figure 9). The inlet capture surface area is designated with a-b, both in Figure 8 and Figure 9. The downstream boundary consists of the nozzle exit plane. By considering this control volume, the aerodynamic forces on the inlet compression surfaces (i.e. the inlet cone of the axi-symmetric configuration and the lower side of the waverider body in front of the inlet cowl lip), are taken into account implicitly and must therefore not be included within the calculations of the external aerodynamic forces.

For on-design intake operation, the book-keeping procedure for evaluating the air flow impulses entering and leaving the boundaries of the control volume and adding up the pressure forces acting on the boundaries of the control volume, yields the following expressions for the internal flow induced forces acting on the vehicle (see Figures 7, 8 and 9):

$$F_l = m_a\left(V_e - V_0\cos(\alpha)\right) + \left(p_e - p_0\right)A_e$$
$$F_n = m_a V_0 \sin(\alpha)$$

The fact that the internal flow is rotated downwards in order to become aligned with the body main axis gives rise to a normal force acting on the vehicle structure. The assumption of ideal expansion (see Section 2.3) has been left. The values of capture area and nozzle exit area determine the extent of flow expansion within the nozzle, which leads to a nozzle exit plane static pressure p_e that is not necessarily equal to the ambient pressure p_0.

At zero angle-of-attack the inlet capture area for on-design inlet operation is designated with cc in Figure 8 and ab' in Figure 9. Flying at a positive angle-of-attack, while maintaining on-design inlet operation, clearly affects the amount of inlet air mass flow capture differently for the two configurations. For the axi-symmetric weapon configuration the inlet air mass flow capture decreases with increasing angle-of-attack (ab < cc; see Figure 8), while for the waverider weapon configuration the inlet mass flow capture increases with increasing angle-of-attack (ab > ab'; see Figure 9). The effect of angle-of-attack on the amount of inlet mass flow capture has been taking into account for the system analyses.

Once equilibrium has been found, vehicle performance can be calculated. The momentary range is used here which is defined as the cruise flight velocity multiplied by the linear estimation of the maximum motor burn time, which is the fuel mass divided by the fuel mass flow rate. For the latter the value at start of the cruise flight is used. The decrease of the fuel mass flow rate during flight due the decrease of the vehicle weight is not taken into account. This can be justified by the objective to assess influences of design choices and model uncertainties on the range and not so much to predict accurately the absolute value of the range. At small angles of attack, for which the equilibrium of forces can be approximated by $F_l = D$ and $L = W$ (see Figure 7), the momentary range can be elegantly separated into a product of the velocity, the structural efficiency, the aerodynamic efficiency, and the engine performance:

$$R = V\frac{M_f}{m_f} = V\frac{M_f}{M_c}\frac{W_c}{m_f g} \approx V\frac{M_f}{M_c}\frac{L}{D}\frac{F_l}{m_f g} = V\varepsilon_m\frac{L}{D}I_{sp}$$

In this equation, ε_m is the structural efficiency, defined as the fuel mass divided by the total mass. For the system analyses the value of 0.1 has been assumed.

2.5 System Performance Analyses

2.5.1 Aerodynamic Efficiency

The first analyses concern the aerodynamic characteristics of both configurations. The figures presented in this section show the lift over drag ratio as function of angle-of-attack at different Mach numbers and show the points on the L/D curves where flight equilibrium is reached (lift equal to vehicle weight).

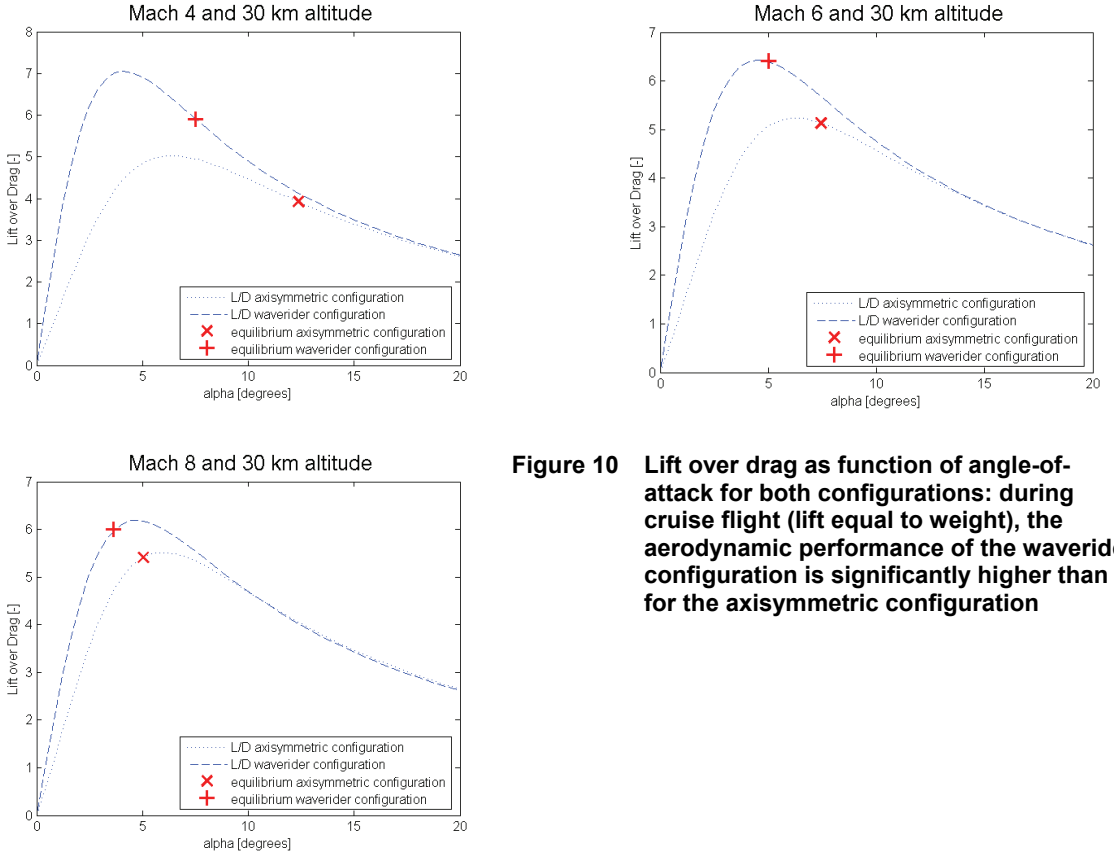

Figure 10 Lift over drag as function of angle-of-attack for both configurations: during cruise flight (lift equal to weight), the aerodynamic performance of the waverider configuration is significantly higher than for the axisymmetric configuration

In Figure 10 it can be seen that for a given angle-of-attack the waverider configuration has a lift over drag ratio that is higher than for the axi-symmetric configuration. The waverider configuration induces more lift

than the axi-symmetric configuration at a given angle-of-attack and therefore the equilibrium angle-of-attack (lift equal to vehicle weight) for the waverider configuration is lower than for the axi-symmetric configuration. For both configurations the equilibrium values of lift over drag are rather close to the optimum values for the Mach number range and altitude of interest (4 < Mach < 8; altitude of 30km). The waverider has a significantly better aerodynamic performance (higher L/D) than the axi-symmetric configuration.

The behaviour of Lift over Drag as function of angle-of-attack can be explained by expressing the lift and drag as follows:

$$\left.\begin{aligned} Lift &= N\cos(\alpha) \\ Drag &= D_0 + N\sin(\alpha) \end{aligned}\right\} \frac{Lift}{Drag} = \frac{N\cos(\alpha)}{D_0 + N\sin(\alpha)}$$

At small angles-of-attack (α < 5º), the total amount of drag is dominated by the zero lift drag D_0. However, the normal force induced drag increases quadratically with the angle-of-attack and will dominate the total amount of drag at larger angles-of-attack (α > 10º). For large angles-of-attack, the lift over drag ratio will therefore approximate the function 1/tanα, independent of freestream conditions and cruise weapon geometry.

At zero angle-of-attack, the lift over drag ratio equals zero of course. At small angles-of-attack the lift increases linearly with angle-of-attack while the drag remains approximately constant due to the very slow increase of the normal force induced drag around zero-angle-of-attack. The lift over drag ratio therefore increases linearly with angle-of-attack for small angles-of-attack. As the normal force induced drag becomes more significant at larger angles-of-attack the lift over drag ratio increase with angle-of-attack becomes less strong, reaches a maximum and starts to approximate the function 1/tanα.

State-of-the-art airbreathing supersonic cruise weapon systems, fly at lower than 30 km altitude at which the waverider type of cruise vehicle does not have a better aerodynamic performance than the conventional axi-symmetric configuration. This can be seen in Figure 11.

The higher dynamic pressure at 10km compared with 30km, implies lower required angles-of-attack for equilibrium flight (lift equal to weight). Both vehicles require the same amount of lift (i.e. both vehicles have the same weight) and due to the better aerodynamic lift characteristics of the waverider it requires a lower angle-of-attack than the axi-symmetric configuration. Because of the relative low angles-of-attack that are required for both vehicles, the aerodynamic drag is dominated by the zero lift drag. An equivalent amount of zero lift drag for both vehicles, therefore means that the lift over drag ratio of both vehicles does not differ much. In general it can be concluded that for small angles-of-attack, there is no reason to choose a waverider configuration over an axi-symmetric one.

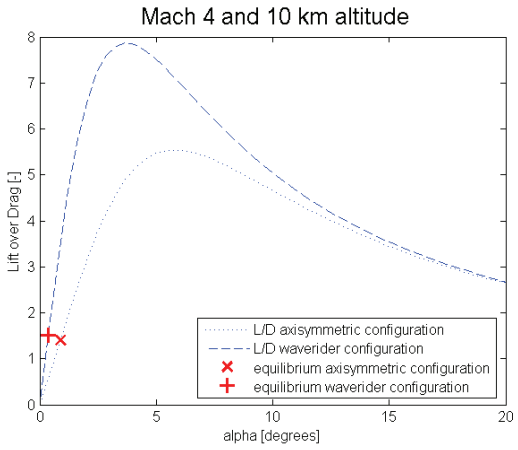

Figure 11 At small angles of attack, L/D values for waverider and axi-symmetric configuration are very close

2.5.2 WAVERIDER versus AXI-SYMMETRIC Configuration; RAMJET engine

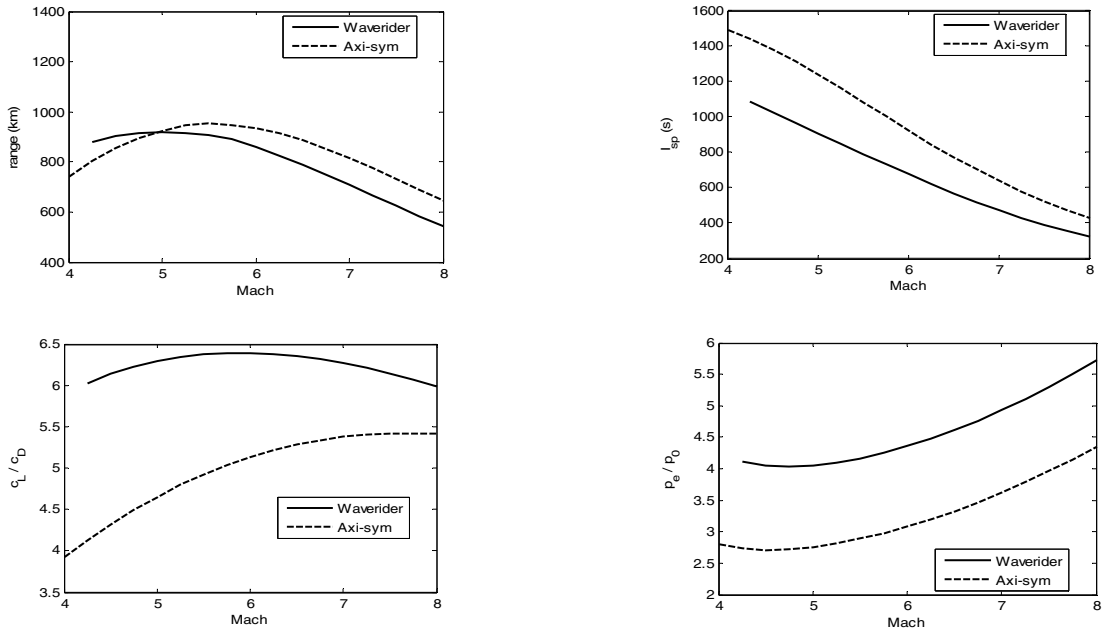

Figure 12 HyTEC analysis results for the waverider and axisymmetric type configurations both equipped with a ramjet engine

As can be seen in Figure 12, the range of both vehicles is close to each other. Apparently the superior aerodynamic performance of the waverider compared with the axisymmetric vehicle is counteracted by a lower engine performance. This is confirmed by the plot for the specific impulse which indeed shows a better engine performance for the axisymmetric configuration. This can be explained by the fact that the waverider reference vehicle increases its effective capture area with angle of attack contrary to the axi-symmetric vehicle which decreases its effective capture area with angle-of-attack (see Figures 8 and 9). This results in an overall effective expansion ratio (A_e/A_0) that is lower for the waverider vehicle compared with the axi-symmetric vehicle. This effect is most pronounced at low Mach numbers where angles of attack are high. For both vehicles the expansion ratio is below ideal expansion (i.e. $p_e/p_0 > 1$, see Figure 12).

2.5.3 RAMJET versus SCRAMJET Engine; WAVERIDER configuration

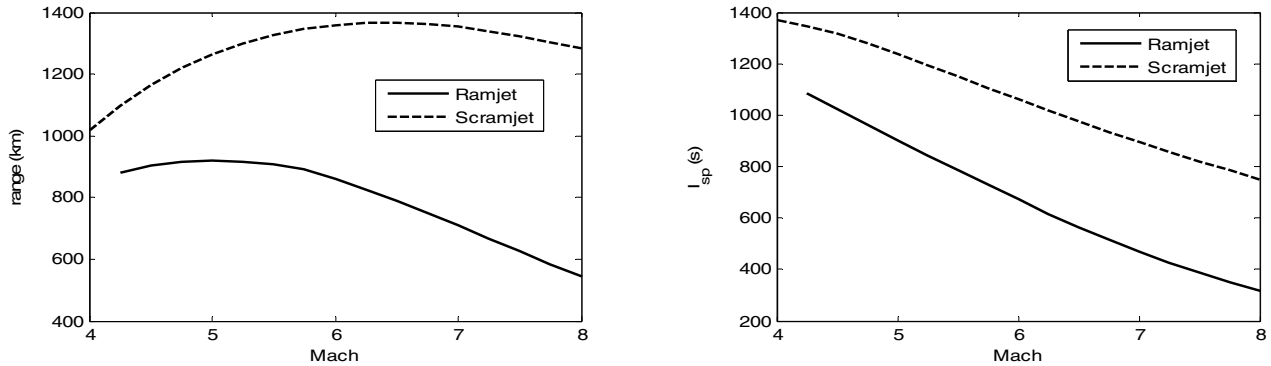

Figure 13 HyTEC analysis result for the waverider configuration; difference between ramjet and scramjet engine

The range that is shown in Figure 13 is, for this case, completely dominated by engine performance as for

both cases (ramjet and scramjet) the vehicle configuration (waverider) and outer dimensions are the same. In other words, the aerodynamic performance between the two cases does not differ.

The scramjet engine has a clear advantage over the ramjet engine at higher Mach numbers (i.e. higher specific impulse). One of the reasons for this is the fact that the ramjet air intake becomes very inefficient at higher Mach numbers. Furthermore, the ramjet loses more thermal energy through dissociation than the scramjet does. Apparently, the lower total pressure losses inside a ramjet combustion chamber compared with a scramjet combustion chamber do not fully compensate for this.

2.5.4 Decreasing the CAPTURE AREA of the WAVERIDER; RAMJET versus SCRAMJET

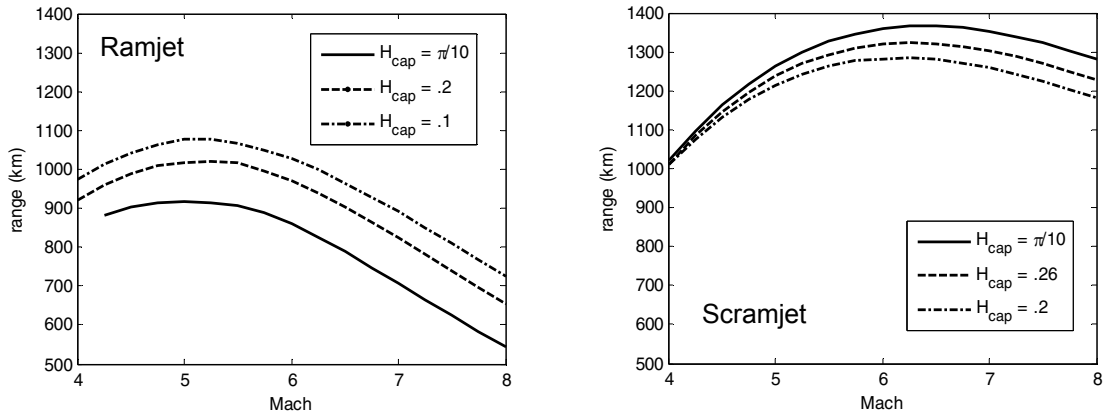

Figure 14 Effect of decreasing the capture area of the waverider on the cruise flight range

A smaller capture area could be beneficial for both configurations, but probably especially for the waverider (see Figure 12, expansion of the hot gases in the nozzle which is significantly above ideal expansion). Lowering the capture area, leads to an increase of the aerodynamic drag because of the introduction of cowl surfaces that experience pressure drag. On the other hand, a lower capture area implies a higher expansion ratio of the internal mass flow (i.e. a lower nozzle exit pressure).

Apparently, the scramjet apparently performs best with a maximum capture area, while ramjet engine performs best at a smaller capture area (see Figure 14).

Apparently, the two counteracting mechanisms on the range of the increase of aerodynamic drag and the increase of motor performance when decreasing the capture area have a negative net effect for the scramjet engine, and a positive net effect for the ramjet engine. For the ramjet engine, the larger expansion ratio results in more performance gain, when compared with the scramjet engine (see Figure 15).

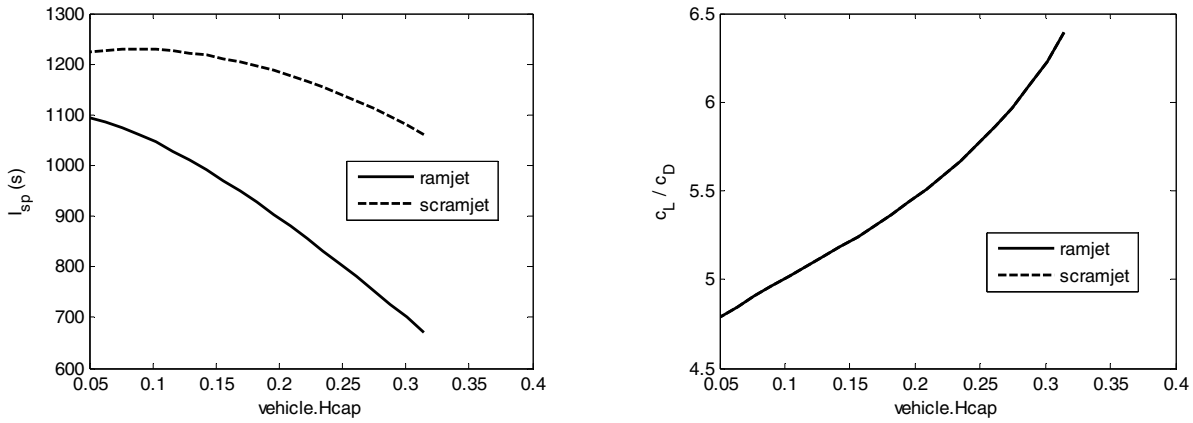

Figure 15 Waverider at Mach 6: Specific impulse increases with decreasing capture area due to the higher expansion ratio, while the lift over drag ratio decreases due to the increasing external cowl surface

2.5.5 Influence of η_K for the AXI-SYMMETRIC Configuration; RAMJET versus SCRAMJET

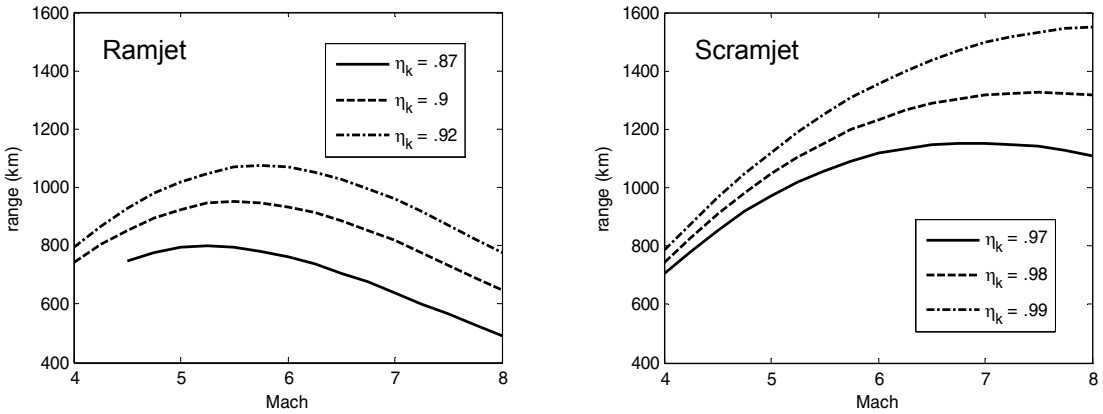

Figure 16 Influence on intake performance on range for the axisymmetric configuration

The influence of η_k on the performance are very large, especially for the scramjet at the higher Mach numbers (see Figure 16). Accurate modelling of intake performance is required in order to be able to accurately predict system performance.

2.5.6 Influence of M2 for the AXI-SYMMETRIC Configuration; SCRAMJET Engine

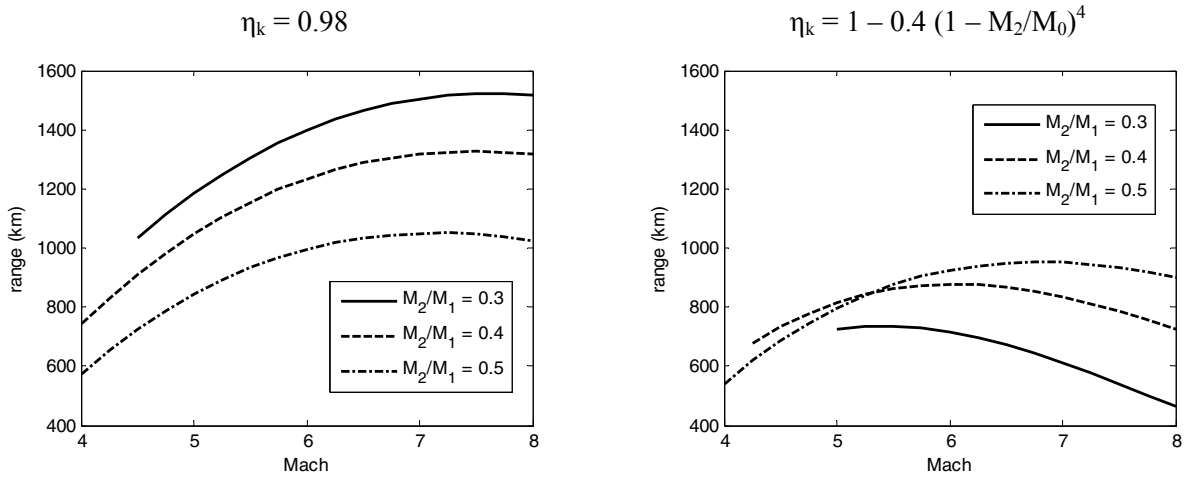

Figure 17 Influence of scramjet mixing chamber Mach number on performance, for different assumptions for intake efficiency

The graphs in Figure 17 show clearly that one should be careful about making conclusions about variations on sub-model parameters. A lower M_2 in itself is beneficial for performance, but will in reality influence the intake efficiency. This can even lead to reversal of the effect. In Figure 16, two different assumptions for η_k are used, both from the same source. Depending on the assumption, the effect of varying M_2 on the performance is quite different.

2.5.7 Influence of DISSOCIATION for the AXI-SYMMETRIC Configuration; RAMJET Engine

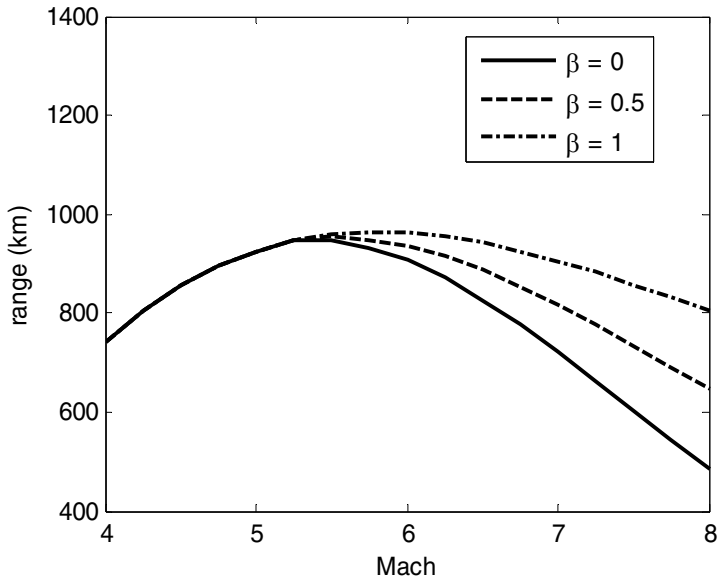

Figure 18 Influence on performance of recombination of dissociated gasses inside the nozzle of the axi-symmetric configuration with ramjet engine.

Figure 18 shows the influence of a 100% variation of β on the performance of the ramjet engine. For ramjets, dissociation becomes significant above Mach 5. At very high Mach numbers, it can decrease the range by almost 50%. For scramjets at the reference flight conditions, where the heating value is quite

low, and static temperatures in the combustion chamber are also low, no dissociation occurs, and variations in the value of β therefore make no difference (not shown in Figure 18, but also the outcome of HyTEC calculations).

2.5.8 Influence of CRUISING ALTITUDE for the AXI-SYMMETRIC Configuration; SCRAMJET Engine

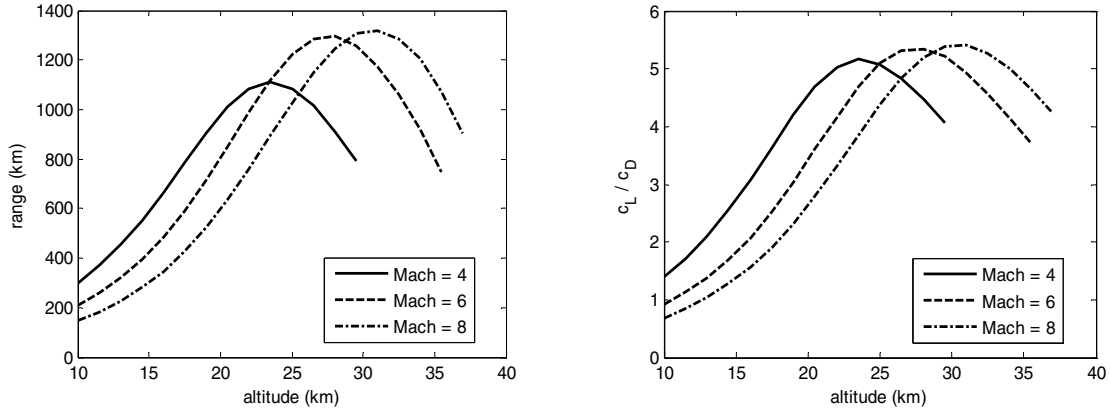

Figure 19 Influence of flight parameter choices for Mach number and cruising altitude on the performance of an axi-symmetric scramjet.

It is apparent from Figure 19 that range increases with altitude up to a maximum. The performance as a function of altitude is mainly aerodynamically driven. At low altitude, the equilibrium angle-of-attack is low and the corresponding lift over drag ratio is far left from the optimum value. When increasing the altitude, dynamic pressure decreases which implies an increase in angle-of-attack. This is accompanied by an increase of lift over drag which is beneficial for the range. Beyond a certain altitude, the angle-of-attack becomes larger than the optimum value.

3.0 CASE STUDY - CRUISE FLIGHT PERFORMANCE OF 1/6 SCALED RAMJET OR ROCKET PROPELLED X-15 CONFIGURATION

Figure 20 1/6 SCALED RAMJET OR ROCKET PROPELLED X-15 CONFIGURATION which could e.g. be considered for a precision hypersonic cruise strike missile

Representation of this configuration by the HyTEC generic axi-symmetric missile configuration (see Figure 3) has been accomplished by matching of the X-15 (1/6 scaled version) overall length and diameter

and matching of the X-15 (1/6 scaled version) total lifting surface (wings, fins and side fairings) with the accompanying values for the generic axisymmetric HyTEC configuration.

Figure 22 shows the results of the first evaluations. For the equilibrium angle-of-attack one can observe a decrease with increasing dynamic pressure caused by either a decreasing cruise flight altitude or increasing cruise flight Mach number.

Angles-of-attack are well below 10 degrees →cruise flight lift over drag is lower than optimal (see Figure 21).

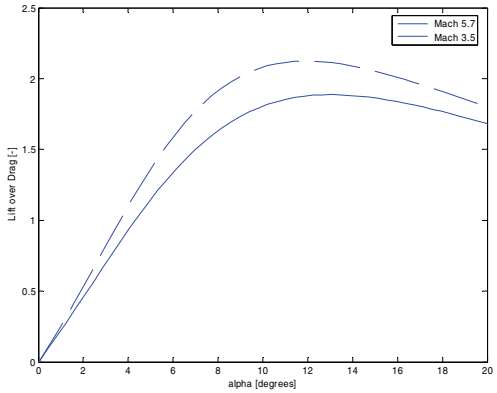

Figure 21 X-15 (1/6 scaled version) lift over drag as function of angle-of-attack for two cruise flight Mach numbers. The optimum lies above 10 degrees angle-of-attack

The higher the altitude and the lower the Mach number,

→ the larger the equilibrium angle-of-attack

→ the larger the cruise flight lift over drag ratio

As range is proportional to lift over drag, therefore the trends of lift over drag can be seen to be reflected in the trends of the range with altitude and Mach number.

The amount of heat that needs to be added per kg of ingested air increases with

- Mach number: drag is proportional to V^2
- Altitude: caused by the increase of induced drag with altitude due to the increasing required angle-of-attack

This limits the maximum altitude that can be reached to around 35km for cruise flight speeds beyond Mach 6. The theoretical boundary for q/cpT0 is determined by the stoichiometric mixture ratio of fuel and air.

Going to higher cruising altitudes would probably be beneficial for system performance (i.e. range) since the larger required angles-of-attack would imply operating the vehicle closer to its optimal lift over drag ratio. A means to lower the required amount of heat to be added to the ingested air is lowering the aerodynamic drag (by lowering wing and fin thickness to chord ratio). Figure 23 shows HyTEC analysis

results for a lower wing and fin thickness to chord ratio.

Higher altitudes are achievable due to the lower vehicle drag. At 40 km and around Mach 4 to 5, the vehicle operates close to its maximum lift over drag.

Another trend that becomes clearly visible now is the decreasing engine specific impulse with altitude

At least two effects contribute to this trend. With increasing altitude:

- the expansion of the hot combustion gases in the nozzle becomes farther away from ideal expansion
- the total combustion temperature increases, exceeding the temperature at which dissociation effects start to extract thermal energy from the internal flow, which for a large part, is not accessible anymore to be converted into kinetic flow energy that is used to generate thrust.

A rocket propelled version has also been examined using HyTEC for which modifications of the code were of course necessary:

- Assuming characteristics of the combustion products representative for a kerosene-H2O2 bi-propellant rocket engine

- Fixed mixture ratio (mean ratio of specific heats = 1.2, mean molar mass = 22 and characteristic velocity = 1640 m/s)
- Maximum combustor pressure of 7 MPa

- The rocket motor exhaust gases expand to the full vehicle body diameter

- The combustor pressure is reduced in case the nozzle exit pressure becomes lower than 0.3 times the ambient pressure in order to prevent nozzle flow separation

- The corresponding thrust coefficient is multiplied with the characteristic velocity and the propellant mass flow rate to yield a thrust

- The propellant mass flow rate is iterated until the horizontal thrust force equals the vehicle drag.

The predicted results (see Figure 24) indicate that a Mach 6 cruise at 40 km altitude may result in cruise flight ranges around 700 km for a rocket propelled vehicle compared to roughly 1800 km for the ramjet propelled vehicle.

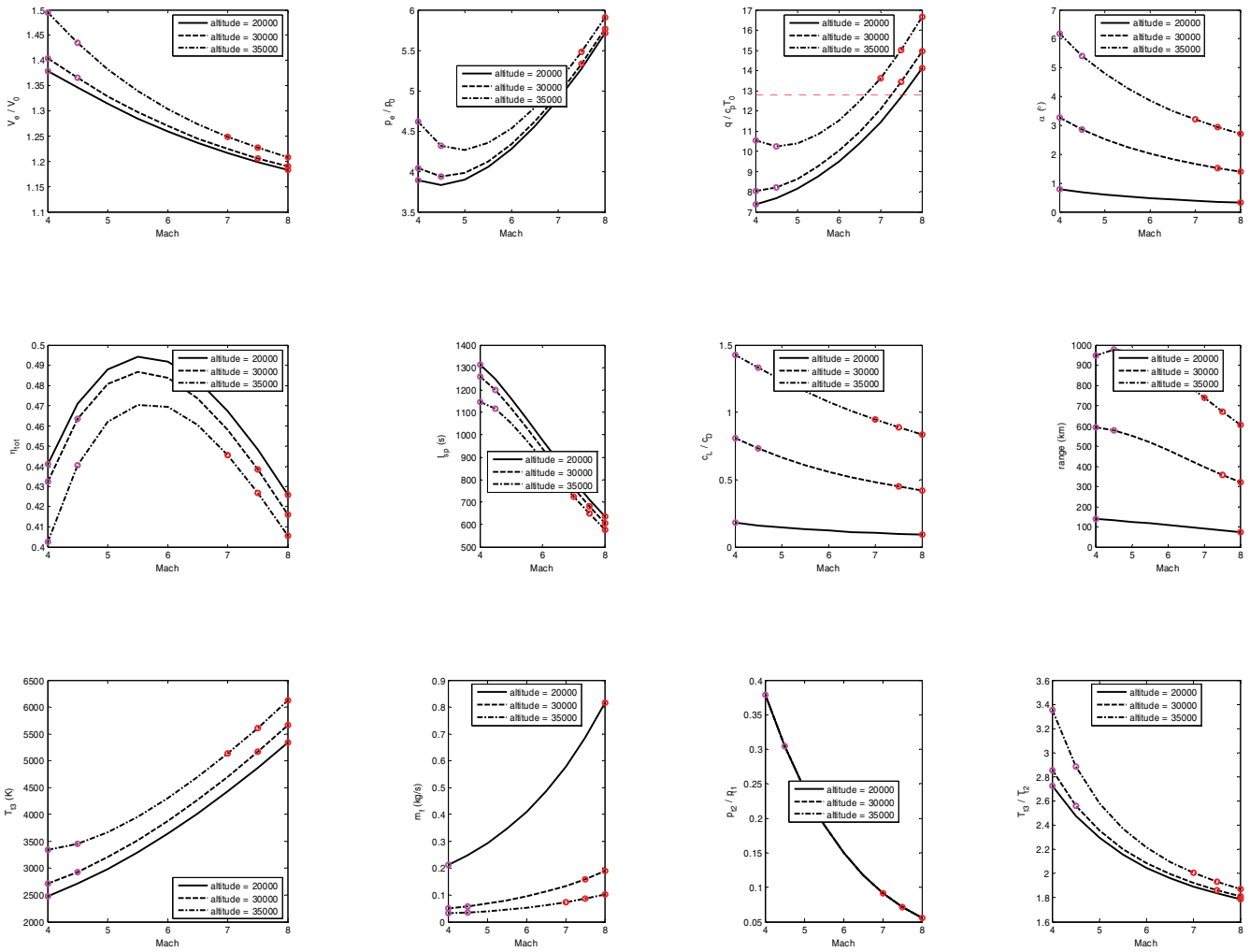

Figure 22 HyTEC cruise flight performance evaluation of a ramjet propelled 1/6 scaled X-15 (Vehicle density = 438 kg/m^3, vehicle mass = 62 kg, t/c = 0.15, Intake capture diameter = vehicle body diameter)

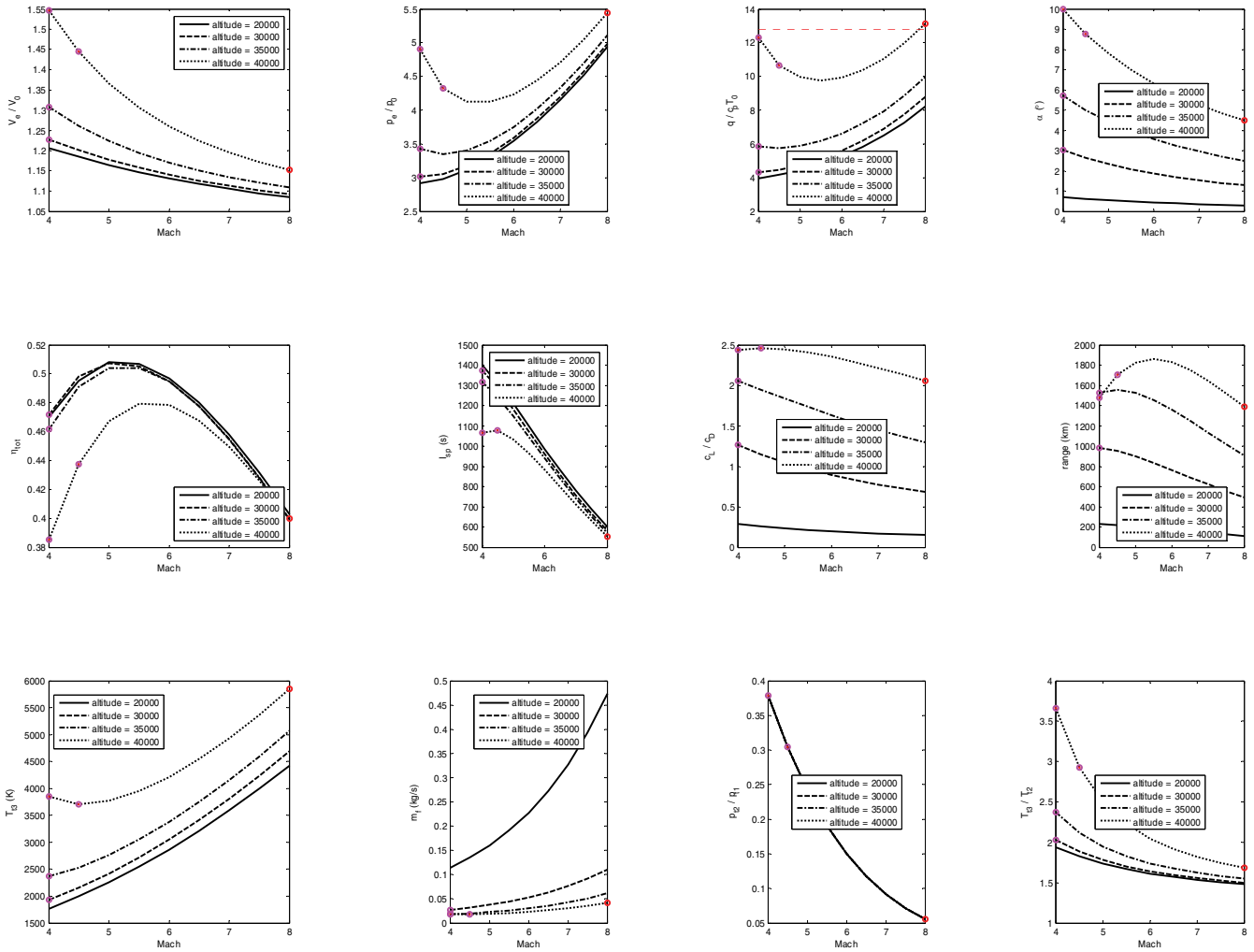

Figure 23 HyTEC cruise flight performance evaluation of a ramjet propelled 1/6 scaled X-15 (Vehicle density = 438 kg/m^3, vehicle mass = 62 kg, t/c = 0.1, Intake capture diameter = vehicle body diameter)

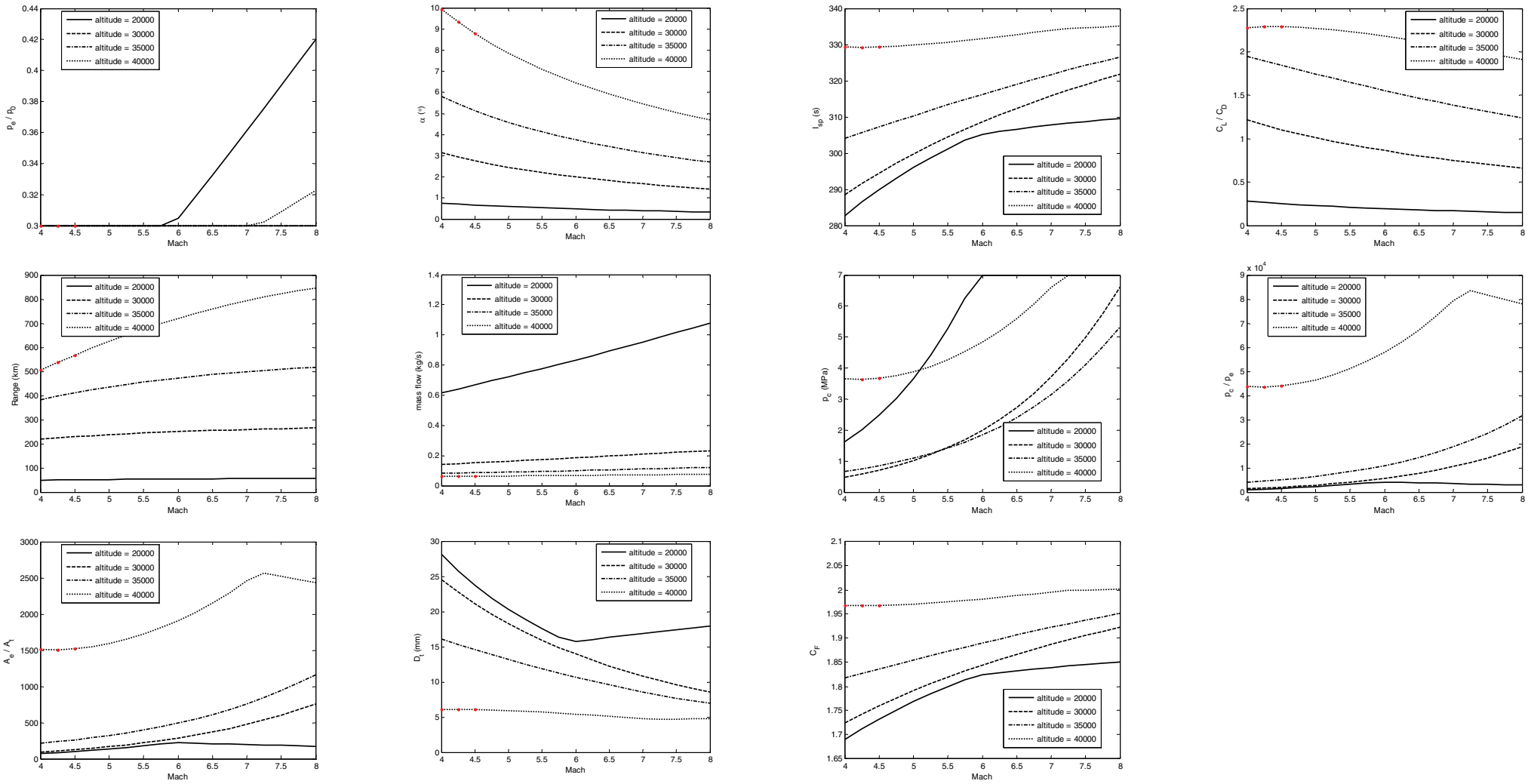

Figure 24 HyTEC cruise flight performance evaluation of a rocket propelled 1/6 scaled X-15 (Vehicle density = 438 kg/m^3, vehicle mass = 62 kg, t/c = 0.1)

4.0 FUTURE EXTENSIONS TO THE HYTEC ANALYSIS TOOL

The estimation of vehicle mass is very rudimentary now in HyTEC:

Vehicle mass = average missile density * internal vehicle volume

For the axi-symmetric vehicle configuration, improved models have been generated for

- the conical air intake
- the cylindrical body

The improved models are described in [3]. They are not yet integrated in HyTEC.

This chapter shows some results for the conical air intake. The conical air intake consists of (see Figure 25):

- Thin walled outer load bearing shell (A)
- Insulation material (C)
- Payload (D, e.g. warhead and GPS/INS hardware)

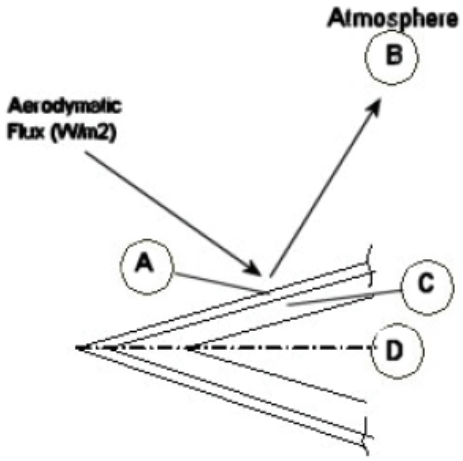

Figure 25 Sketch of the conical air intake [3]

Models for sizing the dimensions of outer shell and insulation are based on:

- Required structural integrity of the outer shell
  - Aerodynamic lift and drag forces taking into account material properties as function of temperature because of aerodynamic heating
- Protection of payload against aerodynamic heating

Aerodynamic heating calculations are based on:

- Taylor-Maccoll method for compressible inviscid cone flow
- Reynolds-analogy for heat transfer from the outer flow to the conical intake shell via the

boundary layer

- Calculation of steady state temperatures determined by the equilibrium of
  - the aerodynamic heat flow
  - radiative cooling
  - heat conduction through the internal structure (in radial direction)
- Constant payload temperature assumed → payload temperature rise or required cooling capacity

Figures 26, 27 and 28 show some results of the aerodynamic calculations.

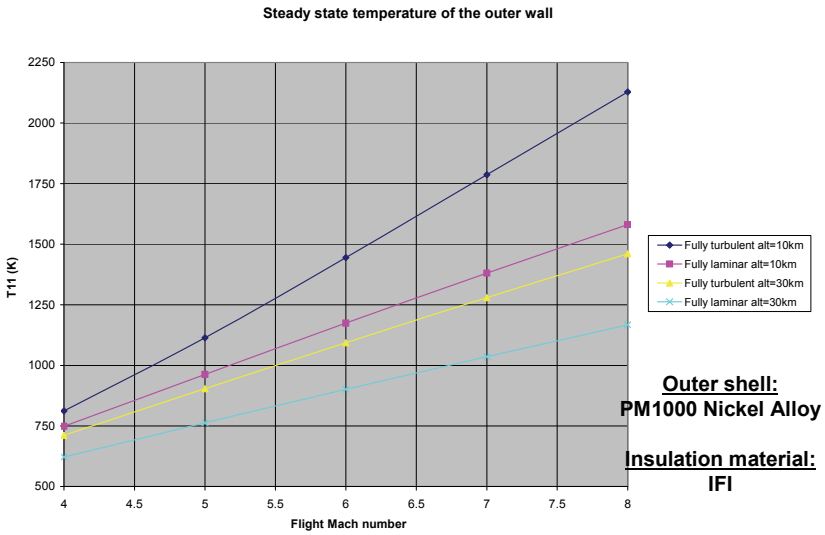

Figure 26 The steady state temperature increases obviously with cruise flight Mach number. Furthermore the cruise flight altitude and the state of the boundary layer determine the steady state temperatures to a large extent. At 10 km, a fully turbulent boundary layer seems reasonable while at 30 km a fully laminar boundary layer is reasonable [3]

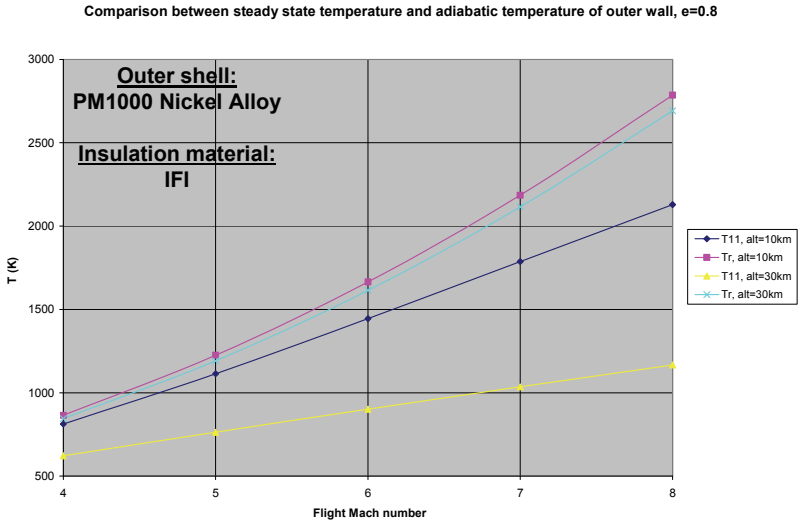

Figure 27 Although the total temperature of the freestream flow does not differ very much between cruise flight at 10km or 30km. However, the differences in the steady state temperatures are significant. These differences are caused by the different states of the boundary layer (laminar at 30km and turbulent at 10 km altitude) and the much lower aerodynamic heating at 30km compared with 10km altitude because of the much lower air density [3]

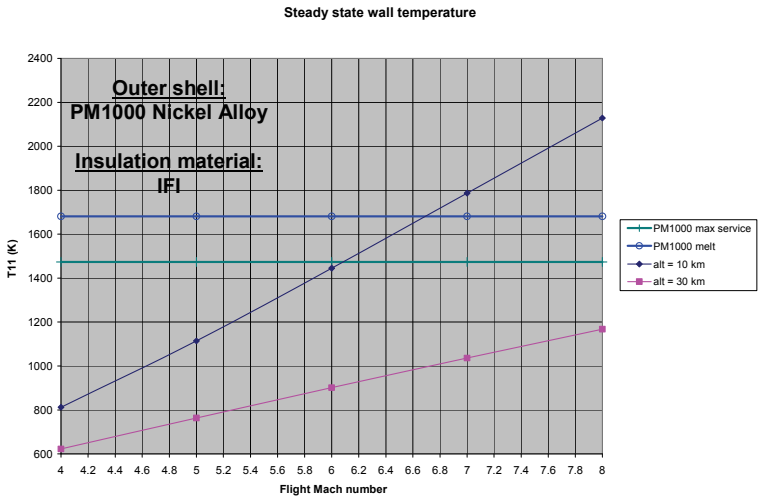

Figure 28 For the PM1000 Nickel Alloy, a cruise flight at 10km altitude is limited to Mach 6 [3]

The structural analysis of the load bearing outer conical shell is based on:

- Several buckling and material failure (yield stress) mechanisms are considered

- Material properties as function of temperature are taken into account

- Loads are the aerodynamic lift and drag forces. These are determined by the cruise Mach number and altitude and the equilibrium angle-of-attack (lift = vehicle weight)

Buckling mechanisms appear to be determining minimal required shell wall thickness [3].

REFERENCES

[1] J.L.P.A. Moerel and Wouter Halswijk (TNO Defence, Security and Safety, Rijswijk, The Netherlands), *'System Analysis of High Speed, Long Range Weapon Systems'*, Published for AIAA Atmospheric Flight Mechanics Conference and Exhibit 2005 – AIAA 2005-5819

[2] J.L.P.A. Moerel and W.H.C. Halswijk (TNO Defence, Security and Safety, Rijswijk, The Netherlands), *'High Speed, Long Range Missiles – System Concepts and Integration',* Paper presented during the NATO RTO-MP-AVT-135 conference on Innovative Missile systems, Amsterdam, the Netherlands, 15-18 May 2006

[3] A.J. van der Star, Aerothermomechanic Analyses of an Axi-symmetric Hypersonic Air Breathing Cruise Missile, final thesis for the Aeronautics study at the INHOLLAND University Delft, February 5, 2008